Precision Calculation of Hyperfine Structure and the Zemach Radii of $^{6,7}Li^+$ Ions

Xiao-Qiu Qi,[1,2,*] Pei-Pei Zhang,[1,3,*] Zong-Chao Yan,[4,1,5] G. W. F. Drake,[3] Zhen-Xiang Zhong,[1,†] Ting-Yun Shi,[1,5] Shao-Long Chen,[1] Yao Huang,[1] Hua Guan,[1,‡] and Ke-Lin Gao[1,5]

[1]*State Key Laboratory of Magnetic Resonance and Atomic and Molecular Physics, Wuhan Institute of Physics and Mathematics, Innovation Academy for Precision Measurement Science and Technology, Chinese Academy of Sciences, Wuhan 430071, China*

[2]*University of Chinese Academy of Sciences, Beijing 100049, China*

[3]*Department of Physics, University of Windsor, Windsor, Ontario, Canada N9B 3P4*

[4]*Department of Physics, University of New Brunswick, Fredericton, New Brunswick, Canada E3B 5A3*

[5]*Center for Cold Atom Physics, Chinese Academy of Sciences, Wuhan 430071, China*

(Received 18 July 2020; accepted 17 September 2020; published 28 October 2020)

The hyperfine structures of the 2^3S_1 states of the $^6Li^+$ and $^7Li^+$ ions are investigated theoretically to extract the Zemach radii of the ^6Li and ^7Li nuclei by comparing with precision measurements. The obtained Zemach radii are larger than the previous values of Puchalski and Pachucki [Phys. Rev. Lett. **111**, 243001 (2013)] and disagree with them by about 1.5 and 2.2 standard deviations for ^6Li and ^7Li, respectively. Furthermore, our Zemach radius of ^6Li differs significantly from the nuclear physics value, derived from the nuclear charge and magnetic radii [Phys. Rev. A **78**, 012513 (2008)] by more than 6σ, indicating an anomalous nuclear structure for ^6Li. The conclusion that the Zemach radius of ^7Li is about 40% larger than that of ^6Li is confirmed. The obtained Zemach radii are used to calculate the hyperfine splittings of the 2^3P_J states of $^{6,7}Li^+$, where an order of magnitude improvement over the previous theory has been achieved for $^7Li^+$.

DOI: 10.1103/PhysRevLett.125.183002

Introduction.—High-precision atomic physics measurements [1–7] and associated theory [8–10] are playing a rapidly increasing role as a probe for both nuclear structure and new physics. In addition to helium, the Li^+ ion is a promising candidate to probe the distribution of magnetic moment inside the nucleus as characterized by the Zemach radius [11]. Recent work on hyperfine structure (hfs) for the ground state of neutral lithium [12] suggested a large unexplained discrepancy for the Zemach radius of ^6Li, as opposed to relatively good agreement for ^7Li. Their results showed that, although the nuclear charge radius of ^7Li is smaller than ^6Li, the Zemach radius is about 40% larger than ^6Li, which is inconsistent with the nuclear data value, as cited by Yerokhin [13]. The analysis depends critically on the theory of hyperfine structure for the isotopes ^6Li and ^7Li, including higher-order relativistic and quantum electrodynamic (QED) effects up to the $m\alpha^6$ limit of current technology. From this, one can determine the Zemach radius as a variable parameter in comparing theory with experiment.

The present work is motivated by an analysis of the recent experimental results for the hfs of $^7Li^+$ of Guan *et al.* [14], as well as by the ongoing experiment on $^6Li^+$ in our laboratory at Wuhan. Following earlier work [15–20], their measurements represent a major step forward in precision for the fine and hyperfine structure for the 2^3S_1 and 2^3P_J states of $^7Li^+$, with uncertainties of less than 100 kHz. These experimental activities will present an important opportunity to probe the nuclear structure of lithium isotopes, particularly for the existing large discrepancy between theory and experiment in the Zemach radius of the ^6Li nucleus. We calculate here the hyperfine splittings of the 2^3S_1 and 2^3P_J states of $^6Li^+$ and $^7Li^+$ with QED corrections included up to order $m\alpha^6$, and find a similarly large disagreement with experiment for the Zemach radius of ^6Li.

The advantage of working with the Li^+ ion is that it is a two-electron system for which highly accurate nonrelativistic wave functions in Hylleraas coordinates are available [21], and so this is removed as a source of uncertainty for all practical purposes. The relativistic corrections of order $m\alpha^4$ to the hfs of $^{6,7}Li^+$ were calculated by Drake and co-workers [19], including the contributions from the nuclear electric quadrupole moment and other nuclear structure effects, and the theoretical accuracy is submegahertz and megahertz, respectively. For the parallel two-electron case of ^3He, the hyperfine structures of the 2^3S_1 and 2^3P_J states were studied by Pachucki *et al.* [22,23], including the QED corrections up to order $m\alpha^6$. Their calculations for 2^3P_J improved the previous theoretical predictions by an order of magnitude.

Theoretical method.—The nonrelativistic quantum electrodynamic theory for quasidegenerate states is used to calculate fine and hyperfine structure splittings [23–26]. In order to obtain the energies of the $2^3\chi_J^F$ ($\chi = S$ or P) states, where the energy level diagram is shown in Fig. 1, we need to diagonalize the effective Hamiltonian H with its matrix elements being

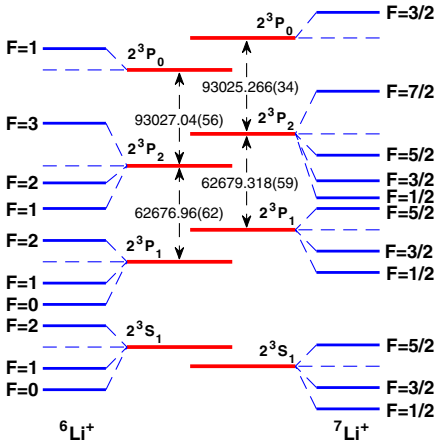

FIG. 1. Hyperfine energy levels (not drawn to scale) of the 2^3S_1 and 2^3P_J states of $^{6,7}Li^+$ [10,19], in MHz.

$$E^F_{JJ'} \equiv \langle JFM_F|H|J'FM_F\rangle, \tag{1}$$

where M_F is the projection of the total angular momentum F, which can be fixed arbitrarily since the energies are independent of it. For convenience, we treat the 2^3P_J centroid as a zero level. The above matrix elements (1) can be expanded in powers of the fine structure constant α:

$$\begin{aligned} E^F_{JJ'} = {} & \langle H_{\rm fs}\rangle_J\delta_{JJ'} + \langle H^{(4+)}_{\rm hfs}\rangle + \langle H^{(6)}_{\rm hfs}\rangle \\ & + 2\langle H^{(4)}_{\rm hfs}, [H^{(4)}_{\rm nfs} + H^{(4)}_{\rm fs}]\rangle + \langle H^{(4)}_{\rm hfs}, H^{(4)}_{\rm hfs}\rangle \\ & + \langle H^{(6)}_{\rm QED}\rangle + \langle H^{\rm ho}_{\rm QED}\rangle + \langle H_{\rm nucl}\rangle + \langle H_{\rm eqm}\rangle, \end{aligned} \tag{2}$$

where $\langle A, B\rangle \equiv \langle A[1/(E_0 - H_0)']B\rangle$, with H_0 and E_0 being the nonrelativistic Hamiltonian and its eigenvalue. $H_{\rm fs}$ is the effective operator that does not depend on the nuclear spin and is responsible for the fine structure splittings [10,19]. The other terms in Eq. (2) are the nuclear spin dependent contributions. $H^{(4+)}_{\rm hfs}$ is the leading-order hyperfine Hamiltonian of $m\alpha^4$, where the superscript + means the higher-order terms from the recoil and anomalous magnetic moment effects. $H^{(6)}_{\rm hfs}$ is the effective operator for the hyperfine splittings of order $m\alpha^6$. $H^{(4)}_{\rm fs}$ and $H^{(4)}_{\rm nfs}$ are the Breit Hamiltonians of order $m\alpha^4$ with and without electron spin. The fifth term in Eq. (2) is the second-order hyperfine correction, which contributes to the isotope shift, fine and hyperfine splittings. $H^{(6)}_{\rm QED}$ and $H^{\rm ho}_{\rm QED}$ are the two effective operators for the QED corrections of order $m\alpha^6$ and higher $\sim m\alpha^7$. Finally, $H_{\rm nucl}$ and $H_{\rm eqm}$ represent the nuclear effects due to the Zemach radius and the nuclear electric quadrupole moment. The detailed forms of these operators are given in Secs. I and II of the Supplemental Material [27].

In our calculations, we use the Hylleraas variational technique [21] to determine high-precision wave functions corresponding to the nonrelativistic part of the Hamiltonian, and then calculate the relativistic, QED, and nuclear effects order by order. Two different wave functions with and without the mass polarization term in the nonrelativistic Hamiltonian are generated. In calculating the second-order terms of $m\alpha^6$, the coupling of intermediate states with different symmetries should be included, where some singular terms are treated by including more singular functions in the intermediate states [34]. All the operators in this work can be expressed in terms of the following ten basic angular momentum operators [23]: S^iL^i, I^iL^i, I^iS^i, $\{S^iS^j\}\{L^iL^j\}$, $I^iS^j\{L^iL^j\}$, $I^iL^j\{S^iS^j\}$, $\{I^iI^j\}\{S^iS^j\}$, $\{I^iI^j\}\{L^iL^j\}$, $S^iL^j\{I^iI^j\}$, and $\{I^iI^j\}\{\{S^mS^n\}\{L^kL^l\}\}^{ij}$, where $S^iL^i \equiv \vec{S}\cdot\vec{L}$, $\{S^iS^j\}$ is the second-order tensor part defined by $\{S^iS^j\} \equiv \frac{1}{2}S^iS^j + \frac{1}{2}S^jS^i - \frac{1}{3}\vec{S}^2\delta^{ij}$, and the summation over

TABLE I. The Zemach radii of $^6Li^+$ and $^7Li^+$. For each ion, two values of the Zemach radius are extracted based on two different transitions, in MHz. In the table, $E_{\rm theor}$ represents the theoretical value of the hfs without the contribution of nuclear structure and R_e is the nuclear charge radius.

	$^6Li^+$		$^7Li^+$	
	$2^3S^0_1 - 2^3S^1_1$	$2^3S^1_1 - 2^3S^2_1$	$2^3S^{1/2}_1 - 2^3S^{3/2}_1$	$2^3S^{3/2}_1 - 2^3S^{5/2}_1$
$E_{\rm theor}$	3002.597(22)	6005.279(14)	11 894.581(69)	19 825.291(46)
$E_{\rm expt}$, Kowalski *et al.* [18]	3001.780(50)	6003.600(50)		
$E_{\rm expt}$, Guan *et al.* [14]			11 890.088(65)	19 817.696(42)
$(E_{\rm expt} - E_{\rm theor})/E_{\rm expt}$	−272(18) ppm	−280(9) ppm	−378(8) ppm	−383(3) ppm
Puchalski and Pachucki [12]	−261(3) ppm		−368(3) ppm	
Yerokhin [13]	−368(60) ppm		−369(23) ppm	
Li *et al.* [12,36]	−277(7) ppm			
$R_{\rm em}$, this work	2.40(16) fm	2.47(8) fm	3.33(7) fm	3.38(3) fm
$R_{\rm em}$, Puchalski and Pachucki [12]	2.30(3) fm		3.25(3) fm	
$R_{\rm em}$, nuclear physics [13]	3.71(16) fm		3.42(6) fm	
$R_{\rm em}$, Li *et al.* [12,36]	2.44(6) fm			
R_e, Lu *et al.* [37]	2.589(39) fm		2.444(44) fm	

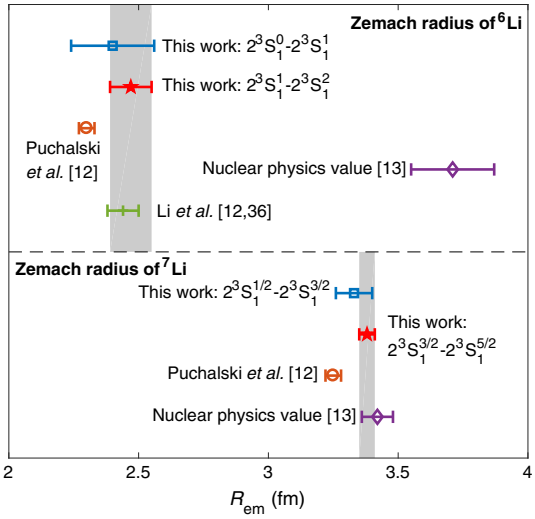

FIG. 2. Comparison of the Zemach radii of ^{6}Li and ^{7}Li.

the repeated indices is assumed. The matrix elements of these operators can be evaluated analytically using Racah algebra.

Zemach radii.—A combination of the experimental [14,18] and theoretical results for the hfs of the 2^3S_1 state can be used to determine the contribution of nuclear structure and extract the Zemach radii. Numerical values of the relevant operators are presented in Sec. III of the Supplemental Material [27]. Our results are given in Table I. Since the theoretical uncertainties of our calculations are mainly from the order $m\alpha^7$ term $H^{\rm ho}_{\rm QED}$, they are taken to be 10% of this contribution calculated approximately; see the Supplemental Material [27]. Two determinations of the Zemach radii from the ^{6,7}Li$^+$ ions are obtained independently based on two different transitions, which are in good agreement with each other. The uncertainty of the Zemach radius from the $2^3S_1^0 - 2^3S_1^1$ transition of ^{6}Li$^+$ is larger, which is caused by the accuracy of experimental measurements. For ^{7}Li$^+$, we also combined our theoretical calculations with the experimental values from Kowalski *et al.* [18] and derived the two Zemach radii 3.38(6) and 3.39(3) fm, which are consistent with those in Table I extracted from the measurements of Guan *et al.* [14]. Thus, we choose 2.47(8) fm for ^{6}Li and 3.38(3) fm for ^{7}Li as the final recommended values of the Zemach radii. An important feature to note is that, to a good approximation, $(E_{\rm expt} - E_{\rm theor})/E_{\rm expt}$ for an S state is directly related to the nuclear Zemach radius, where $E_{\rm theor}$ is the theoretical value without inclusion of the nuclear term, i.e.,

$$\frac{E_{\rm expt} - E_{\rm theor}}{E_{\rm expt}} = \frac{-2ZR_{\rm em}}{a_0}. \tag{3}$$

In other words, this relation is valid for both neutral ^{6,7}Li and ionic ^{6,7}Li$^+$. Also in the table are the values derived by Yerokhin from the nuclear charge and magnetic radii [13].

TABLE II. Theoretical results for individual $2^3P_J^F$ levels in ^{6,7}Li$^+$, relative to the 2^3P_J centroid energy, where the first error in each entry is due to the fine structure and the second error is due to the hyperfine structure, in MHz. The Zemach radius used is 2.47(8) fm for ^{6}Li$^+$ and 3.38(3) fm for ^{7}Li$^+$.

^{6}Li$^+$		^{7}Li$^+$	
$2^3P_0^{F=1}$	103 646.261(612)(1)	$2^3P_0^{F=3/2}$	104 395.489(54)(6)
$2^3P_2^{F=3}$	13 371.488(283)(27)	$2^3P_2^{F=7/2}$	21 709.266(27)(53)
$2^3P_2^{F=2}$	9243.564(283)(14)	$2^3P_2^{F=5/2}$	9936.263(27)(15)
$2^3P_2^{F=1}$	6385.602(283)(40)	$2^3P_2^{F=3/2}$	327.952(27)(52)
$2^3P_1^{F=2}$	−50 782.508(350)(14)	$2^3P_2^{F=1/2}$	−5875.456(27)(79)
$2^3P_1^{F=1}$	−53 670.888(350)(14)	$2^3P_1^{F=5/2}$	−47 679.845(33)(27)
$2^3P_1^{F=0}$	−54 988.619(350)(27)	$2^3P_1^{F=3/2}$	−57 646.278(33)(20)
		$2^3P_1^{F=1/2}$	−61 885.185(33)(45)

Figure 2 shows a comparison of the resulting Zemach radii. Our Zemach radius for ^{7}Li agrees with the nuclear physics value, whereas our result for ^{6}Li disagrees by 6σ (standard deviations) from the value of 3.71(16) fm. Furthermore, our values are all larger than those of Puchalski and Pachucki [12] by 1.5σ and 2.2σ for ^{6}Li and ^{7}Li, respectively. However, their Zemach radii were extracted using the experimental values of Beckmann *et al.* [35]. If instead we combine the most recent measurement of ^{6}Li by Li *et al.* [36] with the calculation of Puchalski and Pachucki, the Zemach radius of ^{6}Li turns out to be 2.44(6) fm, which is in agreement with our result, as shown in Table I and Fig. 2. Our results confirm the conclusion that the Zemach radius of ^{7}Li is about 40% larger than that of ^{6}Li, as was first pointed out by Puchalski and Pachucki [12].

HFS of 2^3P_J.—We calculate the hfs of the 2^3P_J states using our obtained Zemach radii. Numerical values of the relevant operators are shown in Sec. IV of the Supplemental Material [27]. Since the contribution from the $1s$ electron dominates higher-order QED correction, the assumption $H^{\rm ho}_{\rm QED}(1s2p) \simeq H^{\rm ho}_{\rm QED}(1s)$ is used. The uncertainty of this correction is also estimated as 10% of its contribution. According to Eq. (2), the hfs calculations of the 2^3P_J states require the results of the fine structure splittings,

TABLE III. Theoretical hyperfine transitions in the 2^3P_J states of ^{6}Li$^+$, in MHz. In our work, the nuclear electric quadrupole moment used is $Q_d = -0.000806(6) \times 10^{-24}$ cm^2 [41] and the Zemach radius is $R_{\rm em} = 2.47(8)$ fm.

State	(J,F)–(J',F')	Drake and co-workers [19]	This work
2^3P_2	(2,1)–(2,2)	2858.002(61)	2857.962(43)
	(2,2)–(2,3)	4127.882(44)	4127.924(31)
2^3P_1	(1,0)–(1,1)	1317.649(47)	1317.732(31)
	(1,1)–(1,2)	2888.327(29)	2888.379(20)

TABLE IV. Experimental and theoretical hyperfine transitions in the 2^3P_J states of $^7Li^+$, in MHz. In our work, the nuclear electric quadrupole moment used is $Q_d = -0.0400(3) \times 10^{-24}$ cm^2 [41] and the Zemach radius is $R_{em} = 3.38(3)$ fm.

		Experiment			Theory	
State	(J,F)–(J',F')	Kowalski *et al.* [18]	Clarke and van Wijngaarden [20]	Guan *et al.* [14]	Drake and co-workers [19]	This work
2^3P_2	$(2,1/2)$–$(2,3/2)$	6203.6(5)	6204.52(80)	6203.319(67)	6203.27(30)	6203.408(95)
	$(2,3/2)-(2,5/2)$	9608.7(20)	9608.90(49)	9608.220(54)	9608.12(15)	9608.311(54)
	$(2,5/2)$–$(2,7/2)$	11 775.8(5)	11 774.04(94)	11 772.965(74)	11 773.05(18)	11 773.003(55)
2^3P_1	$(1,1/2)-(1,3/2)$	4237.8(10)	4239.11(54)	4238.823(111)	4238.86(20)	4238.920(49)
	$(1,3/2)$–$(1,5/2)$	9965.2(6)	9966.30(69)	9966.655(102)	9966.14(13)	9966.444(34)

which are $\langle H_{fs}\rangle_{J=0} = (8f_{01} + 5f_{12})/9$, $\langle H_{fs}\rangle_{J=1} = (-f_{01} + 5f_{12})/9$, and $\langle H_{fs}\rangle_{J=2} = (-f_{01} - 4f_{12})/9$, relative to the 2^3P_J centroid, with $f_{01} = 155704.00(57)$ MHz and $f_{12} = -62676.96(62)$ MHz for $^6Li^+$ [19] and $f_{01} = 155704.584(48)$ MHz and $f_{12} = -62679.318(59)$ MHz for $^7Li^+$ [10]. The hfs of 2^3P_J of $^6Li^+$ and $^7Li^+$ can be obtained by diagonalizing the matrix in Eq. (2), and the results relative to the 2^3P_J centroid are listed in Table II.

In calculating the second-order energy, we subtract out the dominant $2^1P_1 - 2^3P_1$ singlet-triplet mixing term (ignoring for now hyperfine structure for purposes of illustration) and replace it with the energy shift Δ obtained by exact diagonalization of the corresponding 2×2 Hamiltonian matrix, thereby summing the perturbation series for this term to infinity [38–40] according to the formula

$$\tilde{E} = E - \frac{|\langle 2^3P|H_{mix}|2^1P\rangle|^2}{E(2^3P) - E(2^1P)} + \Delta, \tag{4}$$

where H_{mix} is the singlet-triplet mixing operator. This procedure rapidly becomes essential with increasing Z or with increasing L in order to avoid saturation of singlet-triplet mixing. This modification of the mixing effect alters the hyperfine transitions $(1,1/2)$–$(1,3/2)$ and $(1,3/2)$–$(1,5/2)$ of $^7Li^+$ by 14(2) and 11(3) kHz, respectively. More details are presented in Sec. V of the Supplemental Material [27]. Our results of hfs for $^6Li^+$ and $^7Li^+$ are shown in Tables III and IV. It is noted that the present theoretical values listed in the last column of Table IV improve the previous corresponding ones in Ref. [14] by including the small contributions from the second-order $m\alpha^6$ corrections, as well as by treating the singlet-triplet mixing more rigorously, as mentioned above.

Tables III and IV show that our results have uncertainties less than 100 kHz. The theoretical uncertainty mainly comes from the Zemach radius and the contribution of $m\alpha^7$. For $^6Li^+$, our results are consistent with those of Drake and co-workers [19] at the same level of accuracy. For $^7Li^+$, the calculations of Drake and co-workers [19] have been improved by about one order of magnitude, with the only exception that the value of Drake and co-workers [19] for the $(1,3/2)$–$(1,5/2)$ interval in 2^3P_1 differs from the present calculation. The discrepancy is due to the use of a different value of the nuclear electric quadrupole moment Q_d, because this interval is particularly sensitive to Q_d. It is noted that there is a discrepancy between the experimental value of Guan *et al.* [14] and our calculation for the interval

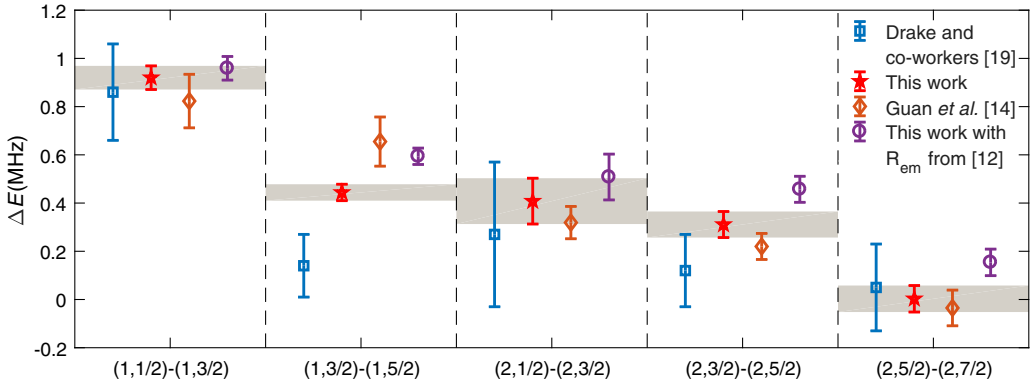

FIG. 3. Comparison of hfs in the 2^3P_J states of $^7Li^+$. ΔE stands for our results for the five indicated transitions relative to 4238, 9966, 6203, 9608, and 11 773, respectively. The blue, red, and purple lines represent the calculations of Drake and co-workers [19], the present calculations using our $R_{em} = 3.38(3)$ fm, and the present calculations using the value of Puchalski and Pachucki [12] $R_{em} = 3.25(3)$ fm, respectively. The brown lines are the experimental results of Guan *et al.* [14].

$(1, 3/2)$–$(1, 5/2)$ of 2^3P_1 of $^7Li^+$, which are only consistent within 1.6σ. We do not have a satisfactory explanation for this discrepancy and we now call for more investigation on the Li^+ isotopes. Figure 3 shows a comparison of hfs transitions of $^7Li^+$. From the figure one can see the influence of the Zemach radius on each transition. For example, for the transition $(1, 3/2)$–$(1, 5/2)$, the result calculated using the Zemach radius of Puchalski and Pachucki [12] is in agreement with the measured value [14], but it disagrees with the measured value for the transition $(2, 3/2)$–$(2, 5/2)$.

Conclusion.—We have studied the hfs of the 2^3S_1 and 2^3P_J states of $^6Li^+$ and $^7Li^+$, including the relativistic and QED corrections up to order $m\alpha^6$. By comparing with the measured hfs of 2^3S_1, we have derived the Zemach radii for the ^6Li and ^7Li nuclei. While the result for ^7Li is in good agreement, the result for ^6Li disagrees by more than 6σ from the value derived from the nuclear charge and magnetic radii by Yerokhin [13], indicating an anomalous nuclear structure for ^6Li. Our results disagree with the previously extracted values from neutral $^{6,7}Li$ [12] by about 1.5σ and 2.2σ, respectively, but they come into agreement for ^6Li when the more recent measurement of hyperfine structure of ^6Li by Li *et al.* [36] is used. Our results also confirm the conclusion [12] that the Zemach radius of ^7Li is about 40% larger than that of ^6Li, even though the charge radius is smaller. Using thus determined Zemach radii, we have calculated the hfs of the 2^3P_J states, where the $2^1P_1 - 2^3P_J$ mixing has been treated rigorously. Our results for the hfs of 2^3P_J in $^7Li^+$ have improved previous calculations by one order of magnitude.

This research was supported by the Strategic Priority Research Program of CAS under Grant No. XDB21010400, and by the National Natural Science Foundation of China under Grants No. 11604369, No. 11774386, No. 11974382, No. 91636216, No. 11934014, and No. 11622434. Z. -X. Z. acknowledges the support from the CAS YIPA program under Grant No. 2017380. H. G. acknowledges the support from the CAS YIPA program under Grant No. Y201963, the Hubei Province Science Fund for Distinguished Young Scholars under Grant No. 2017CFA040, and K. C. Wong Education Foundation under Grant No. GJTD-2019-15. Z.-C. Y. and G. W. F. Drake acknowledge the support from NSERC and SHARCnet of Canada.

*These authors contributed equally to this work.
†zxzhong@wipm.ac.cn
‡guanhua@wipm.ac.cn

[1] P. C. Pastor, L. Consolino, G. Giusfredi, P. De Natale, M. Inguscio, V. A. Yerokhin, and K. Pachucki, Phys. Rev. Lett. **108**, 143001 (2012).
[2] P.-L. Luo, J.-L. Peng, J.-T. Shy, and L.-B. Wang, Phys. Rev. Lett. **111**, 013002 (2013).
[3] X. Zheng, Y. R. Sun, J.-J. Chen, W. Jiang, K. Pachucki, and S.-M. Hu, Phys. Rev. Lett. **118**, 063001 (2017).
[4] K. Kato, T. D. G. Skinner, and E. A. Hessels, Phys. Rev. Lett. **121**, 143002 (2018).
[5] R. J. Rengelink, Y. van der Werf, R. P. M. J. W. Notermans, R. Jannin, K. S. E. Eikema, M. D. Hoogerland, and W. Vassen, Nat. Phys. **14**, 1132 (2018).
[6] S. Schmidt *et al.*, J. Phys. Conf. Ser. **1138**, 012010 (2018).
[7] K. F. Thomas, J. A. Ross, B. M. Henson, D. K. Shin, K. G. H. Baldwin, S. S. Hodgman, and A. G. Truscott, Phys. Rev. Lett. **125**, 013002 (2020).
[8] Z.-C. Yan and G. W. F. Drake, Phys. Rev. Lett. **74**, 4791 (1995).
[9] K. Pachucki, Phys. Rev. Lett. **97**, 013002 (2006).
[10] K. Pachucki and V. A. Yerokhin, Phys. Rev. Lett. **104**, 070403 (2010).
[11] A. C. Zemach, Phys. Rev. **104**, 1771 (1956).
[12] M. Puchalski and K. Pachucki, Phys. Rev. Lett. **111**, 243001 (2013).
[13] V. A. Yerokhin, Phys. Rev. A **78**, 012513 (2008).
[14] H. Guan, S. L. Chen, X. Q. Qi, S. Y. Liang, W. Sun, P. P. Zhou, Y. Huang, P. P. Zhang, Z. X. Zhong, Z. C. Yan, G. W. F. Drake, T. Y. Shi, and K. L. Gao, Phys. Rev. A **102**, 030801(R) (2020).
[15] H. Schüler, Naturwissenschaften **12**, 579 (1924).
[16] B. Fan, A. Lurio, and D. Grischkowsky, Phys. Rev. Lett. **41**, 1460 (1978).
[17] U. Kötz, J. Kowalski, R. Neumann, S. Noehte, H. Suhr, K. Winkler, and G. zu Putlitz, Z. Phys. A **300**, 25 (1981).
[18] J. Kowalski, R. Neumann, S. Noehte, K. Scheffzek, H. Suhr, and G. zu Putlitz, Hyperfine Interact. **15**, 159 (1983).
[19] E. Riis, A. G. Sinclair, O. Poulsen, G. W. F. Drake, W. R. C. Rowley, and A. P. Levick, Phys. Rev. A **49**, 207 (1994).
[20] J. J. Clarke and W. A. van Wijngaarden, Phys. Rev. A **67**, 012506 (2003).
[21] P.-P. Zhang, Z.-X. Zhong, Z.-C. Yan, and T.-Y. Shi, Chin. Phys. B **24**, 033101 (2015).
[22] K. Pachucki, J. Phys. B **34**, 3357 (2001).
[23] K. Pachucki, V. A. Yerokhin, and P. Cancio Pastor, Phys. Rev. A **85**, 042517 (2012).
[24] M. Puchalski and K. Pachucki, Phys. Rev. A **79**, 032510 (2009).
[25] V. Patkóš, V. A. Yerokhin, and K. Pachucki, Phys. Rev. A **100**, 042510 (2019).
[26] M. Haidar, Z.-X. Zhong, V. I. Korobov, and J.-P. Karr, Phys. Rev. A **101**, 022501 (2020).
[27] See Supplemental Material at http://link.aps.org/supplemental/10.1103/PhysRevLett.125.183002 for details of formulas and numerical results, which includes Refs. [28–33].
[28] K. Pachucki, Phys. Rev. A **74**, 022512 (2006).
[29] K. Pachucki and V. A. Yerokhin, J. Phys. Chem. Ref. Data **44**, 031206 (2015).
[30] S. G. Karshenboim and V. G. Ivanov, Eur. Phys. J. D **19**, 13 (2002).
[31] D. K. McKenzie and G. W. F. Drake, Phys. Rev. A **44**, R6973 (1991).

[32] Z.-C. Yan and G. W. F. Drake, Phys. Rev. A **61**, 022504 (2000).
[33] P.-P. Zhang, Z.-X. Zhong, and Z.-C. Yan, Phys. Rev. A **88**, 032519 (2013).
[34] G. W. F. Drake, Can. J. Phys. **80**, 1195 (2002).
[35] A. Beckmann, K. D. Böklen, and D. Elke, Z. Phys. **270**, 173 (1974).
[36] R. Li, Y. Wu, Y. Rui, B. Li, Y. Jiang, L. Ma, and H. Wu, Phys. Rev. Lett. **124**, 063002 (2020).
[37] Z.-T. Lu, P. Mueller, G. W. F. Drake, W. Nörtershäuser, S. C. Pieper, and Z.-C. Yan, Rev. Mod. Phys. **85**, 1383 (2013).
[38] G. W. F. Drake, Phys. Rev. A **19**, 1387 (1979).
[39] D. C. Morton and G. W. F. Drake, Can. J. Phys. **95**, 828 (2017).
[40] A. Wienczek, K. Pachucki, M. Puchalski, V. Patkóš, and V. A. Yerokhin, Phys. Rev. A **99**, 052505 (2019).
[41] N. J. Stone, At. Data Nucl. Data Tables **111–112**, 1 (2016).